^{15}N-^{15}N Proton Assisted Recoupling in Magic Angle Spinning NMR

Supporting Information

Józef R. Lewandowski,[†] *Gaël De Paëpe, Matthew T. Eddy, Robert G. Griffin*[‡]

Department of Chemistry and Francis Bitter Magnet Laboratory, Massachusetts Institute of Technology, Cambridge, Massachusetts 02139, USA.

[†]Current address: Université de Lyon, CNRS/ ENS Lyon/ UCB-Lyon 1, Centre RMN à Très Hauts Champs, 5 rue de la Doua, 69100 Villeurbanne, France

[‡] Corresponding author email: rgg@mit.edu

Atom	X	Y	Z	δ_{iso} (ppm)	δ_{aniso} (ppm)	η
$N_{35}N$	6.433	0.681	21.962	-5	-106	0.2
$N_{35}H$	5.718	1.142	21.364	0	5.7	0.65
$D_{36}N$	5.419	-1.641	23.313	5	-110	0.2
$D_{36}H$	4.904	-1.32	22.468	0	5.7	0.65

Table SI1. Atom coordinates and chemical shift values of the spin system used in the numerical simulation in the Fig. 2. The coordinates are taken from the x-ray structure of GB1 protein (PDB ID 2GI9). The ^{1}H's were added in Chimera[81] and NH bonds adjusted to 1.04 Å in Accelrys DS Visualizer 2.0.

Atom	X	Y	Z	δ_{iso} (ppm)	δ_{aniso} (ppm)	η
$K_{31}N$	3.707	3.18	17.231	-5	-106	0.2
$Q_{32}N$	2.57	1.986	19.467	5	-110	0.2
$Y_{33}N$	3.579	-0.659	18.994	1	-106	0.2
$A_{34}N$	6.33	-0.189	19.299	3	-110	0.2
$K_{31}H$	2.982	3.7	16.696	5	5.7	0.65
$Q_{32}H$	1.892	2.273	18.733	0	5.7	0.65
$Y_{33}H$	3.186	-0.156	18.173	0	5.7	0.65
$A_{34}H$	5.812	0.508	18.727	0	5.7	0.65

Table SI2. Atom coordinates and chemical shift values for the α-helix spin system used in simulation in Fig. 5. The coordinates are taken from the x-ray structure of protein GB1 (PDB ID 2GI9) and NH bonds adjusted to 1.04 Å in Accelrys DS Visualizer 2.0.

Atom	X	Y	Z	δ_{iso} (ppm)	δ_{aniso} (ppm)	η
$T_{43}N$	11.226	9.874	16.505	-5	-106	0.2
$T_{44}N$	10.639	9.569	12.975	5	-106	0.2
$T_{45}N$	8.75	10.166	9.967	2	-106	0.2
$T_{53}N$	10.547	5.747	11.227	-3	-106	0.2
$V_{54}N$	12.114	4.79	14.309	1	-106	0.2
$T_{43}H$	10.945	10.753	16.916	0	5.7	0.65
$T_{44}H$	10.777	8.569	12.993	0	5.7	0.65
$T_{45}H$	8.907	11.164	9.947	0	5.7	0.65
$T_{53}H$	10.255	6.709	11.323	0	5.7	0.65
$V_{54}H$	12.455	3.893	13.995	0	5.7	0.65

Table SI3. Atom coordinates and chemical shift values for the spin system used in the simulation in Fig. 6b. The coordinates are taken from the x-ray structure of protein GB1 (PDB ID 2GI9) and NH bonds adjusted to 1.04 Å in Accelrys DS Visualizer 2.0.

Atom	X	Y	Z	δ_{iso} (ppm)	δ_{aniso} (ppm)	η
$D_{230}N$	-38.088	27.067	-13.66	-3	-106	0.2
$I_{231}N$	-34.794	26.728	-12.382	-5	-106	0.2
$R_{232}N$	-31.47	27.642	-12.164	1	-106	0.2
$V_{267}N$	-34.544	21.857	-11.351	5	-106	0.2
$V_{268}N$	-31.194	22.88	-11.52	2	-106	0.2
$D_{230}H$	-38.252	27.981	-13.191	0	5.7	0.65
$I_{231}H$	-34.757	25.695	-12.496	0	5.7	0.65
$R_{232}H$	-31.714	28.643	-12.306	0	5.7	0.65
$V_{267}H$	-34.665	20.829	-11.247	0	5.7	0.65
$V_{268}H$	-31.439	23.889	-11.464	0	5.7	0.65

Table SI4. Atom coordinates and chemical shift values for the spin system used in simulation in Fig. 6d. The coordinates are taken from the model 0.1 from the SSNMR structure of HET-s (218-289) prion (PDB ID 2RNM) and NH bonds adjusted to 1.04 Å in Accelrys DS Visualizer 2.0.

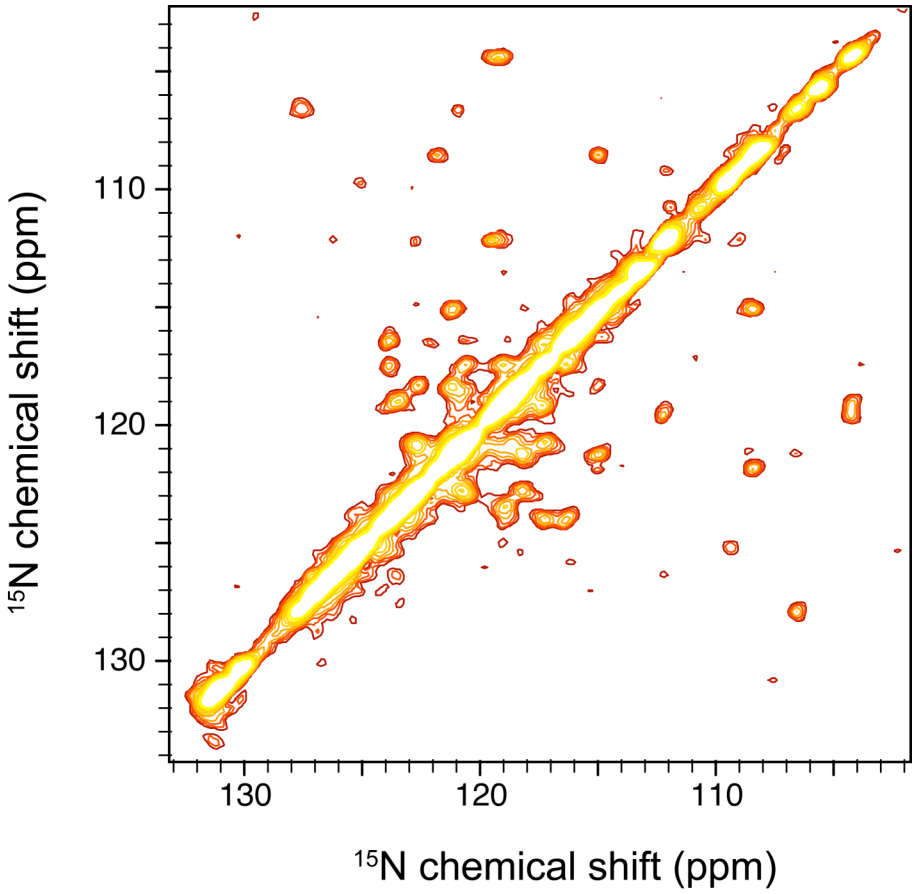

Figure SI1. 2D ^{15}N-^{15}N PAR correlation spectrum on [1,3-^{13}C,U-^{15}N]-protein GB1. The spectrum was obtained using 22 ms PAR mixing with ~ 4 kHz ^{15}N and ~ 52 ^{1}H CW irradiation at $\omega_r/2\pi = 20$ kHz MAS and $\omega_{0H}/2\pi = 900$ MHz.

Assignment	ω_1 (ppm)	ω_2 (ppm)	Assignment	ω_1 (ppm)	ω_2 (ppm)	Assignment	ω_1 (ppm)	ω_2 (ppm)
M1N-Q2N	40.1	125.3	V29N-F30N	119.0	118.3	D46N-D47N	126.8	123.4
L5N-T16N	126.9	115.2	F30N-V29N	118.2	119.0	D46N-T51N	126.4	112.2
L7N-G14N	127.0	105.6	F30N-K31N	118.7	120.6	D47N-D46N	123.3	126.4
N8N-G9N	125.2	109.5	K31N-F30N	120.7	118.6	D47N-A48N	123.5	119.0
G9N-N8N	109.7	125.0	Q32N-K31N	121.2	119.9	A48N-D47N	119.0	123.3
K10N-T11N	121.1	106.6	Y33N-A34N	121.0	122.6	A48N-T49N	118.9	104.1
T11N-K10N	106.5	121.0	A34N-Y33N	122.5	121.0	T49N-A48N	104.4	119.1
T11N-L12N	106.6	127.6	A34N-N35N	122.5	118.1	T49N-K50N	104.4	119.5
L12N-T11N	127.8	106.6	N35N-A34N	118.5	122.7	K50N-T49N	119.4	104.3
G14N-L7N	105.6	127.1	N35N-D36N	118.3	121.2	K50N-T51N	119.5	112.2
T16N-L5N	115.3	126.8	N35N-N37N	118.3	115.0	T51N-D46N	112.3	126.4
A23N-A24N	122.8	120.6	D36N-A34N	121.3	122.5	T51N-K50N	112.3	119.5
A24N-A23N	120.6	122.8	D36N-N35N	121.2	118.2	T51N-F52N	112.3	130.1
A24N-T25N	120.7	117.2	D36N-N37N	121.2	115.0	F52N-T51N	130.3	112.2
A24N-A26N	120.8	123.8	N37N-N35N	115.0	118.1	T53N-T44N	112.2	109.0
T25N-A24N	117.4	120.5	N37N-D36N	115.1	121.1	T53N-V54N	112.3	118.5
T25N-A26N	117.4	123.8	N37N-G38N	115.1	108.4	V54N-T53N	118.5	112.1
A26N-A24N	124.0	120.6	G38N-N37N	108.5	115.0	T55N-E42N	124.1	119.1
A26N-T25N	124.0	117.2	G38N-V39N	108.6	121.7			
A26N-E27N	123.9	116.4	V39N-G38N	121.8	108.4			
E27N-A26N	116.5	123.9	D40N-V39N	131.2	121.6			
E27N-K28N	116.5	117.2	D40N-G41N	131.0	108.2			
K28N-E27N	117.5	116.3	G41N-D40N	108.4	131.2			
K28N-V29N	117.4	118.8	E42N-T55N	119.3	124.0			
V29N-K28N	119.1	117.3	T44N-T53N	109.1	112.1			

Table SI5. Cross-peaks observed in the spectra in Fig. 4. The sequential cross-peaks in the loop regions are highlighted in red, sequential cross-peaks in the α-helix are highlighted in green, and interstrand cross-peaks within the antiparallel β-sheets are highlighted in blue.

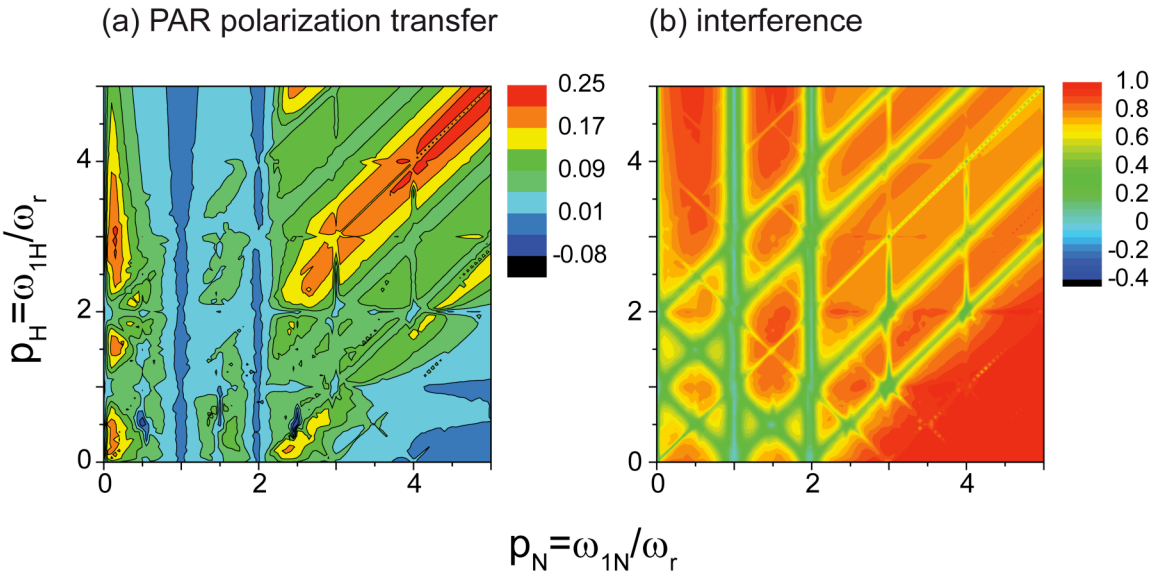

Figure SI2. Comparison of the ^{15}N-^{15}N PAR polarization transfer map (a) and the interference map (b). Simulation was performed for the spin system described in Table SI1 using 20 ms of PAR mixing at $\omega_r/2\pi$=20 kHz MAS and $\omega_{0H}/2\pi$=750 MHz. In the PAR optimization map the polarization transfer between the nitrogens is monitored as a function of nitrogen (p_N) and proton (p_H) irradiation in units of spinning frequency. In the interference map the decay of the magnetization on the nitrogens after the PAR mixing is monitored as a function of nitrogen (p_N) and proton (p_H) irradiation in units of spinning frequency. The initial magnetization is prepared on the x-axis on one of the nitrogens in (a) and on both nitrogens in (b). Usually, one can find the optimal PAR settings by running a small number of 1D interference experiments. First, one needs to identify the rotary resonance conditions by employing high power ^{1}H decoupling and scanning through the ^{15}N rf settings. Then, one can fix the nitrogen power at a desired level and scan through the ^{1}H rf settings in order to identify Hartmann-Hahn conditions. We experimentally observe the interference (rotary resonance and Harmann-Hahn) conditions present in the simulations (both the interference and the polarization transfer maps), which allows us to appropriately orient the rf settings for a PAR mixing period.

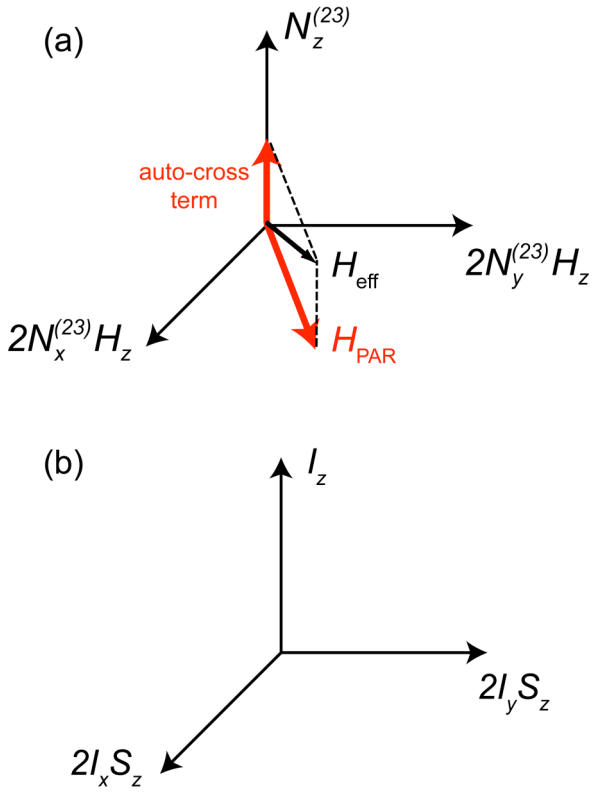

Figure SI3. Visualization of the PAR subspace. The space can be seen as a coupled basis between a fictitious ZQ operator involving the two carbons (or nitrogens) and a proton spin. The red arrows indicate PAR recoupling axis and longitudinal tilting field resulting from auto-cross terms. Panel (b) depicts the coupled basis encountered in solution NMR.

Atom	X	Y	Z	δ_{iso} (ppm)	δ_{aniso} (ppm)	η
$T_{44}N$	10.639	9.569	12.975	-5	-106	0.2
$T_{53}N$	10.547	5.747	11.227	5	-106	0.2
$W_{43}H_{\alpha}$	10.835	8.369	15.129	0	5.7	0.65
$W_{4}H_{\beta 3}$	8.402	9.135	14.812	0	5.7	0.65
$W_{43}H_{\varepsilon 3}$	7.851	6.796	14.29	0	5.7	0.65
$T_{44}H$	10.781	8.539	12.994	0	5.7	0.65
$T_{44}H_{\alpha}$	10.044	11.236	11.893	0	5.7	0.65
$T_{44}H_{\gamma 2}$	13.117	10.317	12.407	0	5.7	0.65
$T_{53}H$	10.246	6.738	11.326	0	5.7	0.65
$T_{53}H_{\gamma 1}$	14.093	7.513	11.659	0	5.7	0.65

Table SI6. Atom coordinates and chemical shift values for the spin system used in simulation in Fig. 7. The coordinates are taken from the x-ray structure of protein GB1 (PDB ID 2GI9) and NH bonds adjusted to 1.04 Å in Accelrys DS Visualizer 2.0.

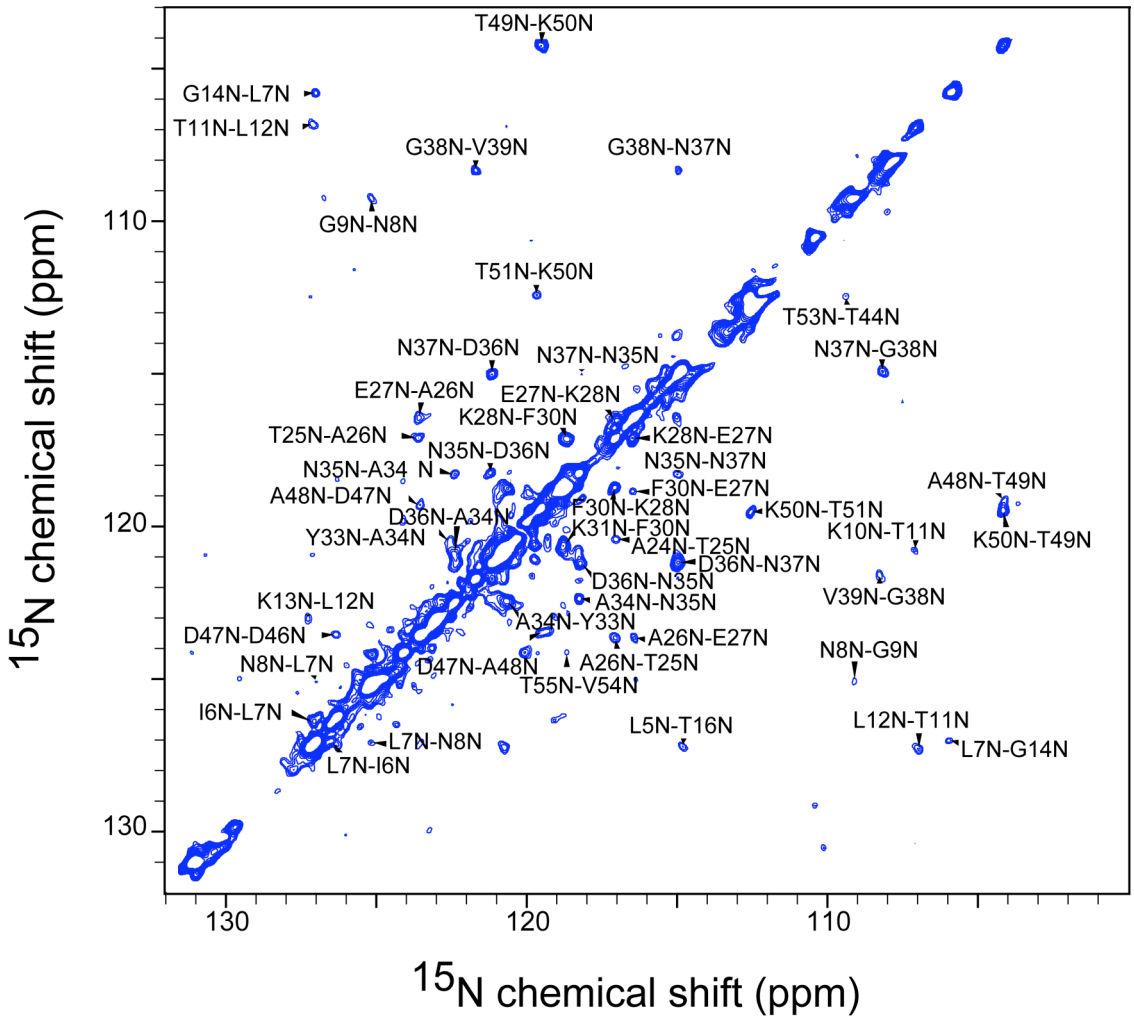

Figure SI4. 2D ^{15}N-^{15}N PAR correlation spectrum on [U-^{13}C,^{15}N]- protein GB1. The spectrum was obtained using 20 ms PAR mixing with ~71 kHz ^{15}N and ~ 69 ^{1}H CW irradiation at $\omega_r/2\pi$=11.11 kHz MAS and $\omega_{0H}/2\pi$=500 MHz. The acquisition time was 46.1 ms in t_1 and 46.1 ms in t_2. The temperature (as read by thermocouple) was maintained at -5°C using 50 scfh flow of nitrogen.

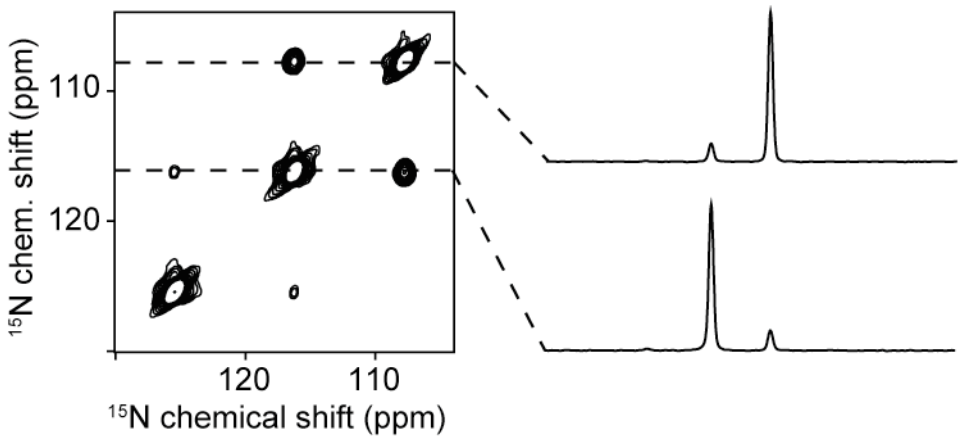

Figure SI5. Slices from the low power 2D ^{15}N-^{15}N PAR correlation spectrum obtained on [U-^{13}C,^{15}N]-*f*-MLF-OH[71] at $\omega_r/2\pi = 20$ kHz and $\omega_{0H}/2\pi = 900$ MHz using 20 ms of mixing time.

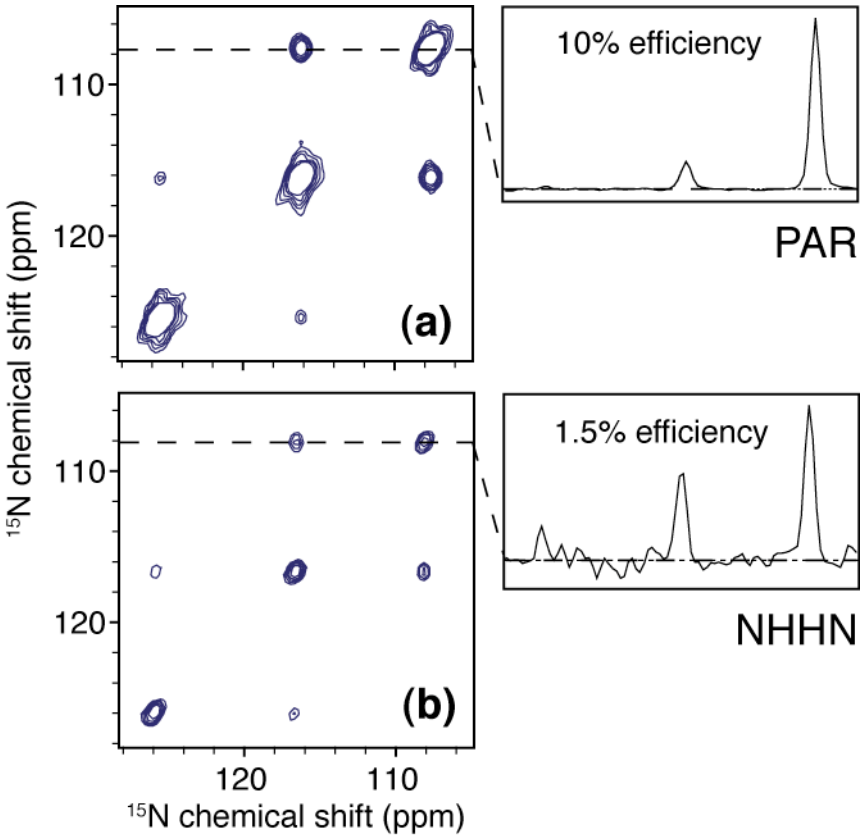

Figure SI6. Comparison of ^{15}N-^{15}N PAR and NHHN on [U-^{13}C,^{15}N]-*f*-MLF-OH. (a) 2D ^{15}N-^{15}N PAR correlation spectrum with 25 ms mixing time. (b) 2D NHHN correlation spectrum with 0.8 ms mixing time. The panels on the right of the spectra show 1D slices at FN frequency. **Note that the slices can be used to judge the relative SNR of the spectra but cannot be used for judging of the polarization transfer efficiency.** Even

though the cross-peak in the NHHN spectrum consists ~60% of the diagonal peak it correlates to only 1.5 % polarization transfer efficiency (compared to a reference experiment with zero mixing time). On the other hand, the cross-peak in the PAR spectrum corresponds to 10 % transfer efficiency even though it consists much smaller fraction of the diagonal peak. Both of the spectra were obtained at $\omega_r/2\pi$ = 20 kHz and $\omega_{0H}/2\pi$ = 750 MHz using the same settings except for the mixing scheme. The spectra were chosen based on the best achievable LN-FN polarization transfer efficiency for the 0.6-1.2 ms mixing time range for NHHN and 5-25 ms mixing time range for PAR.